# $V_{us}$ from $\pi$ and $K$ decay constants in full lattice QCD with physical $u$, $d$, $s$, and $c$ quarks

R. J. Dowdall,[1,2] C. T. H. Davies,[2,*] G. P. Lepage,[3] and C. McNeile[4]

(HPQCD Collaboration)[†]

[1]*DAMTP, University of Cambridge, Wilberforce Road, Cambridge CB3 0WA, United Kingdom*
[2]*SUPA, School of Physics and Astronomy, University of Glasgow, Glasgow G12 8QQ, United Kingdom*
[3]*Laboratory of Elementary-Particle Physics, Cornell University, Ithaca, New York 14853, USA*
[4]*Bergische Universität Wuppertal, Gaussstrasse 20, D-42119 Wuppertal, Germany*

(Received 11 March 2013; published 21 October 2013)

We determine the decay constants of the $\pi$ and $K$ mesons on gluon field configurations from the MILC Collaboration including $u$, $d$, $s$, and $c$ quarks. We use three values of the lattice spacing and $u/d$ quark masses going down to the physical value. We use the $w_0$ parameter to fix the relative lattice spacing and $f_\pi$ to fix the overall scale. This allows us to obtain a value for $f_{K^+}/f_{\pi^+} = 1.1916(21)$. Comparing to the ratio of experimental leptonic decay rates gives $|V_{us}| = 0.22564(28)_{\mathrm{Br}(K^+)}(20)_{\mathrm{EM}}(40)_{\mathrm{latt}}(5)_{V_{ud}}$ and the test of unitarity of the first row of the Cabibbo-Kobayashi-Maskawa matrix: $|V_{ud}|^2 + |V_{us}|^2 + |V_{ub}|^2 - 1 = 0.00009(51)$.

DOI: 10.1103/PhysRevD.88.074504 PACS numbers: 12.38.Gc, 13.20.−v, 14.40.Df

## I. INTRODUCTION

The annihilation of a charged $\pi$ or $K$ meson to leptons via a $W$ boson is a "gold-plated" process whose rate can be determined very accurately from experiment. The decay width for pseudoscalar $P$ made of valence quarks $a\bar{b}$ is given by

$$\Gamma(P \to l\nu) = \frac{G_F^2 |V_{ab}|^2}{8\pi} f_P^2 m_l^2 M_P \left(1 - \frac{m_l^2}{M_P^2}\right)^2 \qquad (1)$$

up to known electromagnetic corrections. Here $V_{ab}$ is the appropriate Cabibbo-Kobayashi-Maskawa (CKM) matrix element for coupling to the $W$ and $f_P$ is the pseudoscalar decay constant which parametrizes the amplitude for the annihilation. $f_P$ can only be determined accurately from lattice QCD calculations.

The experimental determination of $\Gamma(K^+ \to l\nu)/\Gamma(\pi^+ \to l\nu)$ can be converted to a result for the ratio of the CKM element $\times$ decay constant for $K$ and $\pi$. Using experimental averages [1] $\Gamma(\pi^+ \to l\nu) = 3.8408(7) \times 10^7\,\mathrm{s}^{-1}$ and $\Gamma(K^+ \to l\nu) = 5.133(13) \times 10^7\ \mathrm{s}^{-1}$ gives

$$\frac{|V_{us}| f_{K^+}}{|V_{ud}| f_{\pi^+}} = 0.27598(35)_{\mathrm{Br}(K^+)}(25)_{\mathrm{EM}}. \qquad (2)$$

Here we have allowed for an electromagnetic correction to the ratio of widths given by $(1 + \delta_{\mathrm{EM}})$ with $\delta_{\mathrm{EM}} = -0.0070(18)$ [2,3]. The error in Eq. (2) from this correction is sizeable but not as large as that from the $K^+$ branching fraction to $\mu\nu$ which dominates. The total error in determining the ratio of Eq. (2) from experiment is then 0.16%.

The electromagnetic correction means that $f_K$ and $f_\pi$ are defined as quantities in pure QCD without electromagnetic interactions. An accurate theoretical result from lattice QCD for $f_{K^+}/f_{\pi^+}$ then yields $|V_{us}|/|V_{ud}|$ [4]. Since $V_{ud}$ is known accurately from nuclear $\beta$ decay, this gives $V_{us}$. The higher the accuracy on $V_{us}$ the more stringent the test of CKM first row unitarity we can do, since $V_{ub}$ is too small to contribute (at present) to this. Any deviations are indications of new physics and the more stringent the test, the higher the scale to which the new physics is pushed.

State-of-the-art lattice QCD calculations have achieved errors below 1% in $f_K/f_\pi$ [5–9], typically dominated by the systematic errors from extrapolation of the lattice results to the real-world continuum and chiral limits where the lattice spacing is zero and the $u/d$ quark masses take their physical values (equivalent to the $\pi$ meson mass taking its physical value). This means that significant improvements can be expected if we reduce discretization errors, to make the continuum extrapolation more benign, and if we work with physical $u/d$ quark masses that obviate the need for a chiral extrapolation. It also means that the comparison of different methods for arriving at a physical answer from lattice QCD are important in testing systematic error estimates.

The MILC Collaboration recently gave an analysis of $f_{K^+}/f_{\pi^+}$ [10] from lattice QCD on their "second-generation" gluon field configurations that include $u$, $d$, $s$, and $c$ quarks in the sea using the highly improved staggered quark (HISQ) formalism [11] and a fully $\mathcal{O}(\alpha_s a^2)$ improved gluon action [12]. They have ensembles with the average of the $u$ and $d$ quark masses down to the physical value. Their final error was 0.4% on the decay constant ratio dominated by errors from the extrapolation to zero lattice spacing. Their analysis [10] concentrated on the ensembles with physical $u/d$ quark mass and the aim was to perform a single self-contained analysis that did not use additional information from, for example, chiral perturbation theory or determination of the lattice spacing using other quantities.

*c.davies@physics.gla.ac.uk
†http://www.physics.gla.ac.uk/HPQCD

 

In this paper we provide a new analysis with the most accurate result to date. To do this we use the same MILC ensembles with a completely independent analysis of meson correlation functions with high statistics. We include ensembles with heavier-than-physical $u/d$ quark masses and use chiral perturbation theory to pin down the point corresponding to physical light- and strange-quark masses. We also include very accurate information on the relative lattice spacings of the ensembles using the Wilson flow parameter, $w_0$ [13]. This enables us to reduce the error on the decay constant ratio to below 0.2% which is close to the error coming from experiment in Eq. (2).

Section II describes the lattice calculation. The results and analysis, including a table of all our raw lattice values for meson masses and decay constants, are given in Sec. III. This is followed by a discussion and conclusions in Secs. IV and V respectively.

## II. LATTICE CALCULATION

### A. Meson correlators

Table I gives the parameters for the MILC ensembles of gluon field configurations that we use here [14,15]. The table includes the values of sea-quark masses in lattice units, where the $u$ and $d$ quarks are taken to have the same mass, $m_\ell = m_u = m_d$. The accurate determination of the lattice spacing will be discussed further below. Here we simply note that the "very coarse" lattices (sets 1, 2, and 3) have lattice spacing, $a \approx 0.15$ fm, the coarse lattices (sets 4, 5, and 6) have $a \approx 0.12$ fm, and the fine lattices (sets 7 and 8) have $a \approx 0.09$ fm. Thus the spatial volumes of the lattices are large: the sets with physical $m_l$ (sets 3, 6, and 8) are all larger than 4.8 fm on a side, with sets 6 and 8 being larger than 5.5 fm on a side.

On these ensembles we calculate light and $s$-quark propagators using the same HISQ action as used in the sea. The valence $\ell$ quarks are taken to have the same mass as those in the sea, the valence $s$ quarks are retuned slightly to correspond more closely to the physical value [16]. The valence masses used are given in Table III. We use an unsmeared random wall source on each of 16 time sources per configuration for very high statistical accuracy [16].

TABLE I. Details of the MILC gluon field ensembles used in this paper [14,15]. $\beta = 10/g^2$ is the SU(3) gauge coupling and $L$ and $T$ give the length in the space and time directions for each lattice. $am_{\ell,\mathrm{sea}}$, $am_{s,\mathrm{sea}}$, and $am_{c,\mathrm{sea}}$ are the light (up and down taken to have the same mass), strange, and charm sea-quark masses in lattice units. The ensembles 1, 2, and 3 will be referred to in the text as "very coarse," 4, 5, and 6 as "coarse," and 7 and 8 as "fine." The number of configurations that we have used in each ensemble is given in the final column. We have used 16 time sources on every configuration.

| Set | $\beta$ | $am_{\ell,\mathrm{sea}}$ | $am_{s,\mathrm{sea}}$ | $am_{c,\mathrm{sea}}$ | $L/a \times T/a$ | $n_{\mathrm{cfg}}$ |
|---|---|---|---|---|---|---|
| 1 | 5.80 | 0.013 | 0.065 | 0.838 | $16 \times 48$ | 1020 |
| 2 | 5.80 | 0.0064 | 0.064 | 0.828 | $24 \times 48$ | 1000 |
| 3 | 5.80 | 0.002 35 | 0.0647 | 0.831 | $32 \times 48$ | 1000 |
| 4 | 6.00 | 0.0102 | 0.0509 | 0.635 | $24 \times 64$ | 1052 |
| 5 | 6.00 | 0.005 07 | 0.0507 | 0.628 | $32 \times 64$ | 1000 |
| 6 | 6.00 | 0.001 84 | 0.0507 | 0.628 | $48 \times 64$ | 1000 |
| 7 | 6.30 | 0.0074 | 0.0370 | 0.440 | $32 \times 96$ | 1008 |
| 8 | 6.30 | 0.0012 | 0.0363 | 0.432 | $64 \times 96$ | 621 |

The propagators are combined to make meson correlation functions for $\pi$, $K$, and $\eta_s$ mesons. The $\eta_s$ is a fictitious $s\bar{s}$ meson that is not allowed to decay here because we do not include the disconnected pieces of the correlation function. Since it does not contain valence $u/d$ quarks it is a useful particle to study in lattice QCD [16,18]. We include it here to provide more information to our fits about the meson mass dependence of the decay constants.

We average over the 16 time sources to obtain a result for each configuration and then study the configuration-to-configuration correlations. An autocorrelation analysis was performed in [16] and plots of the autocorrelation function for the $\pi$ and $\eta_s$ correlators are given for the ensembles with $m_\ell/m_s = 0.1$ and 0.2. The autocorrelation function for the sets at physical $m_\ell/m_s$ show a decrease in correlation between configurations. We give an example in Fig. 1 for the $\pi$ meson correlator on coarse set 6. The other physical point ensembles show very similar behavior. We bin over two adjacent configurations on sets 1, 2, 3, and 6 and bin over four adjacent configurations on all other sets.

We then fit all three meson correlators simultaneously as a function of time, $t$, between source and sink according to

$$G_{\mathrm{meson}}(t) = \sum_{k=0}^{n_{\mathrm{exp}}} a_k (e^{-E_k t} + e^{-E_k (T-t)}) - (-1)^{t/a} \sum_{ko=0}^{n_{\mathrm{exp}}} \tilde{a}_{ko} (e^{-\tilde{E}_{ko} t} + e^{-\tilde{E}_{ko}(T-t)}). \quad (3)$$

The oscillating piece is absent for the $\pi$ and $\eta_s$ mesons because the valence quark and antiquark have equal mass. We use Bayesian fitting methods [19,20] so that the full effect of excitations in the spectrum can be included in the

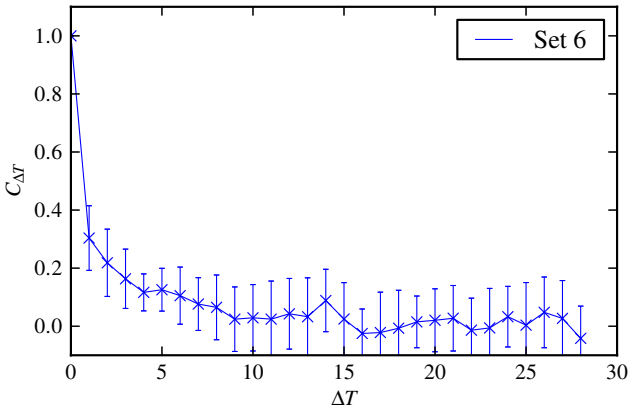


FIG. 1 (color online). The autocorrelation function for the $\pi$ meson correlator at lattice time 20 on coarse set 6. $\Delta T = 1$ corresponds to adjacent configurations in the ordered list for the set which are 5 molecular dynamics time units apart.

errors on the ground-state quantities that we are interested in, i.e. $a_0$ and $E_0$ for each meson. The simultaneous fit to all three mesons allows us to take into account the correlations between the fit results for each meson in our subsequent analysis. Results are taken from six exponential fits (with an additional six oscillating exponentials for the $K$).

The $\pi$, $K$, and $\eta_s$ meson masses are given by the appropriate $E_0$ values from the fit above. The decay constant is determined from the corresponding amplitude, $a_0$, by

$$f_{ab} = (m_a + m_b)\sqrt{\frac{2a_0}{E_0^3}} \tag{4}$$

for a meson with quark content $a\bar{b}$ [5]. This formula holds for Goldstone pseudoscalar mesons made of staggered quarks and follows from the existence of a partially conserved axial current relation in these formalisms. The decay constant is then absolutely normalized in lattice QCD.

Table III gives the results of our correlator fits for the decay constant and meson masses in lattice units on each ensemble. The errors are below 0.1% in almost all cases.

### B. Lattice spacing determination

It has recently been proposed that lattice spacings be measured by smoothing the gluon field using a series of infinitesimal "smearing" steps [13,21]. This drives the gluon field towards a smooth renormalized field and gauge-invariant functions of this field, such as the pure gluon action density, become physical quantities. The parameters used to determine the lattice spacing can then be defined from the flow-time, $t$, dependence of such quantities. Reference [21] defines $t_0$ from

$$t^2\langle E\rangle|_{t=t_0} = 0.3, \tag{5}$$

where $\langle E\rangle$ is the expectation value of the gluon action density. The parameter $w_0$ is preferred in [13], where $w_0$ is defined by

$$t\frac{d}{dt}t^2\langle E\rangle|_{t=w_0^2} = 0.3. \tag{6}$$

$w_0$ should be less sensitive to small flow times where discretization effects may be important. Both $w_0$ and $t_0$ can be determined by direct measurement on the gluon field and this makes them simpler to evaluate as well as typically more precise than parameters based on the heavy-quark potential [22]. The heavy-quark potential must be determined by fitting large Wilson loops as a function of (lattice) time and then, to extract parameters such as $r_1$ [14], a further fit as a function of $r$ must be done to the potential.

None of $w_0$, $t_0$, and $r_1$ can be simply related to any directly measurable experimental quantity and their physical value must be determined by a lattice QCD calculation of such a quantity. For example, $w_0$ and $t_0$ are determined from the mass of the $\Omega$ baryon in [13] and $r_1$ is determined from a basket of quantities including the $\Upsilon$ excitation energy and the decay constant of the $\eta_s$ meson in [16,18].

TABLE II. Values of the lattice spacing for the ensembles of Table I in units of parameters $w_0$ [13], $t_0$ [21], and $r_1$ [23]. The $r_1/a$ values were calculated by MILC and given in [15].

| Set | $w_0/a$ | $\sqrt{t_0}/a$ | $r_1/a$ |
|---|---|---|---|
| 1 | 1.1119(10) | 1.0249(5) | 2.059(23) |
| 2 | 1.1272(7) | 1.0319(3) | 2.073(13) |
| 3 | 1.1367(5) | 1.0357(2) | 2.089(8) |
| 4 | 1.3826(11) | 1.2389(5) | 2.575(17) |
| 5 | 1.4029(9) | 1.2475(4) | 2.626(13) |
| 6 | 1.4149(6) | 1.2521(3) | 2.608(8) |
| 7 | 1.8869(39) | 1.6515(16) | 3.499(24) |
| 8 | 1.9525(20) | 1.6769(7) | 3.565(13) |

Here we will use $w_0/a$ to determine the relative lattice spacing between the ensembles and finally fix its value from $f_\pi$ in our analysis in Sec. III. We give values for $w_0/a$ on each ensemble in Table II and also, for comparison, of $\sqrt{t_0}/a$. These were obtained using the methods explained

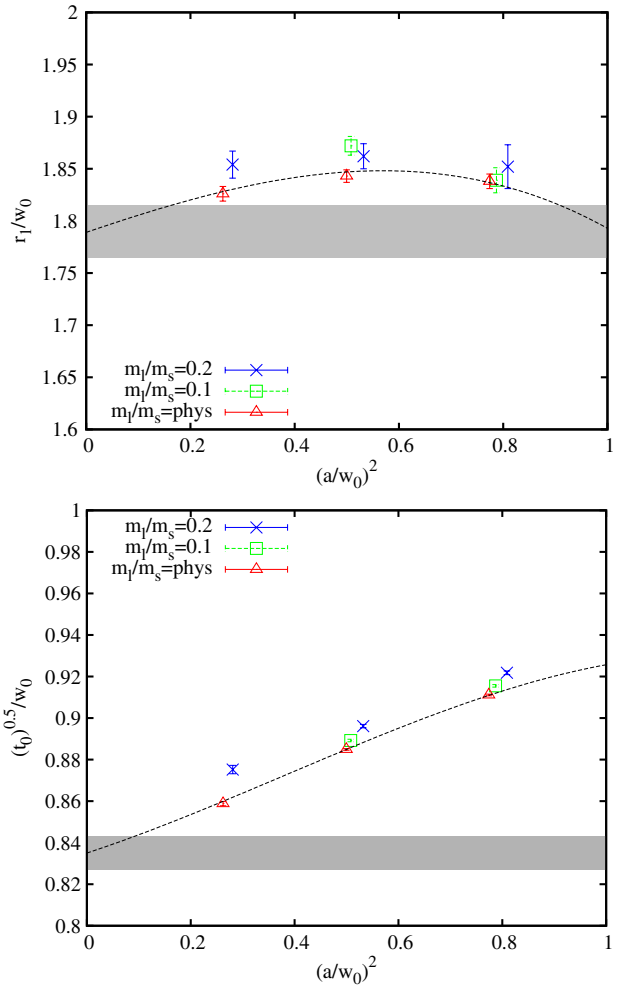


FIG. 2 (color online). At the top the ratio $r_1/w_0$ plotted as a function of $a^2$ and below the ratio $\sqrt{t_0}/w_0$. The grey band gives the results of a simple polynomial fit to the $a^2$ and $m_\ell$ dependence as described in the text. The dashed line shows the fit evaluated at the physical value for $m_l/m_s$ of 0.036 [1].

in [13]. We bin over 12 adjacent configurations (60 molecular dynamics time units on all sets except for set 8 where it is 72 time units) to remove the effects of autocorrelations in the results as assessed by a binning analysis.

Figure 2 compares the scales $w_0$, $t_0$, and $r_1$ by plotting $r_1/w_0$ and $\sqrt{t_0}/w_0$ as a function of $(a/w_0)^2$. We see that discretization errors largely cancel between $r_1$ and $w_0$ since their ratio is very flat in $a^2$. There is a small variation with $m_\ell$. The errors here are dominated by statistical/fitting errors in $r_1$. In contrast $\sqrt{t_0}/w_0$ is much more precise but has relatively strong lattice-spacing dependence, presumably from $\sqrt{t_0}$ [13]. We carried out a simple polynomial fit in $m_\ell/(10m_s)$ and $\alpha_s(\Lambda a)^2$, $(\Lambda a)^4$, $(\Lambda a)^6$ with $\Lambda = 0.6$ GeV for both ratios, taking priors on the coefficients of 0.0(1.0). This gives the result $r_1/w_0 = 1.789(26)$ and $\sqrt{t_0}/w_0 = 0.835(8)$ in the continuum and physical light-quark mass limits represented by the grey shaded bands in Fig. 2. The result for $\sqrt{t_0}/w_0$ agrees well with the BMW-c result of 0.835(15)(7) using the Wilson clover 2-HEX action in [13].

## III. ANALYSIS AND RESULTS

Table III gives our raw lattice results for the pseudoscalar meson masses and decay constants in lattice units. In this section we use these data to compute the dependence of $f_\pi$, $f_K$, and $f_{\eta_s}$ on the quark masses and on the lattice spacing. This allows us to interpolate to the physical values of the strange-quark and light-quark masses, and to extrapolate to zero lattice spacing, obtaining new predictions for the decay constants (as well as the $\eta_s$ mass). The differences between our most chiral simulation data and our final results are small since our simulation is very close to physical. It is nevertheless important to model these corrections accurately to optimize the precision of our final results.

Our analysis involves the following steps:

(1) Remove the lattice spacing by multiplying the masses and decay constants for the $\pi$, $K$, and $\eta_s$ by the values (with errors) of $w_0/a$ from Table II. We also apply an singular value decomposition (svd) cut to the data to guarantee that roundoff errors are not an issue when inverting the covariance matrix for the $\chi^2$ function. This in effect triples the statistical errors.

(2) Fit the simulation results for $w_0 f_\pi$, $w_0 f_K$, $w_0 f_{\eta_s}$, and $w_0^2 M_{\eta_s}^2$, together with the experimental result for $f_{\pi^+}$, as functions of the corresponding pion and kaon masses, and $w_0$. We take the functional dependence from one-loop partially quenched chiral perturbation theory plus terms polynomial in $M_\pi^2$, $M_K^2$, and $a^2$. The fit gives a new value for $w_0$, which is largely determined by the experimental value for $f_\pi$ used in the fit. It also gives the functional dependence of the decay constants and the $\eta_s$ mass on the quark masses, as specified by $M_\pi$ and $M_K$. Sea- and valence-quark masses are specified separately. The same chiral formulas, with the same couplings, are used for pions, kaons, and $\eta_s$s; only the valence-quark masses differ.

(3) Evaluate the best-fit functions for $f_K$ and $f_\pi$ at values of the pion and kaon masses appropriate for $f_{\pi^+}$ and $f_{K^+}$. We set the $u$ and $d$ quark masses equal in our simulations. We correct for this approximation through appropriate choices for the values of $M_\pi$ and $M_K$ used in our fit formulas to obtain our final results. At the same time we correct for (small) electromagnetic corrections to the meson masses. [The decay constants, by definition, do not need electromagnetic corrections; these are included explicitly in Eq. (2).]

In the rest of this section we elaborate on these steps, and survey our results.

### A. Chiral fit

We fit our lattice results for the decay constants using a formula drawn from partially quenched chiral perturbation theory [24] that has the following form:

TABLE III. Values for $\pi$, $K$, and $\eta_s$ masses and decay constants in lattice units calculated for valence masses given in columns 2 and 3. Some of the results were previously given in [16,17]. There are slight differences in some values with earlier results because different fit results were used.

| Set | $am_{\ell,\mathrm{val}}$ | $am_{s,\mathrm{val}}$ | $aM_\pi$ | $af_\pi$ | $aM_K$ | $af_K$ | $aM_{\eta_s}$ | $af_{\eta_s}$ |
|---|---|---|---|---|---|---|---|---|
| 1 | 0.013 | 0.0688 | 0.236 44(15) | 0.111 84(10) | 0.412 14(24) | 0.126 95(15) | 0.533 50(17) | 0.141 85(9) |
| | | 0.0641 | | | 0.400 06(19) | 0.125 85(10) | 0.515 11(16) | 0.140 09(7) |
| 2 | 0.0064 | 0.0679 | 0.166 14(7) | 0.105 08(6) | 0.390 77(10) | 0.122 65(4) | 0.527 98(9) | 0.140 27(4) |
| | | 0.0636 | | | 0.379 48(10) | 0.121 77(4) | 0.510 80(9) | 0.138 40(4) |
| 3 | 0.002 35 | 0.0628 | 0.101 72(4) | 0.099 38(6) | 0.365 57(8) | 0.118 37(4) | 0.506 56(6) | 0.137 20(2) |
| 4 | 0.010 44 | 0.0522 | 0.191 58(9) | 0.090 77(6) | 0.327 89(11) | 0.101 89(5) | 0.423 58(11) | 0.113 18(4) |
| 5 | 0.005 07 | 0.0505 | 0.134 14(6) | 0.084 52(5) | 0.307 56(10) | 0.097 88(4) | 0.414 74(8) | 0.111 19(3) |
| 6 | 0.001 84 | 0.0507 | 0.081 54(2) | 0.079 90(3) | 0.298 43(5) | 0.095 32(2) | 0.414 78(4) | 0.110 65(2) |
| 7 | 0.0074 | 0.0364 | 0.140 62(10) | 0.066 18(5) | 0.239 19(11) | 0.074 24(4) | 0.308 71(10) | 0.082 36(3) |
| 8 | 0.0012 | 0.0360 | 0.057 16(2) | 0.057 84(3) | 0.218 55(5) | 0.069 21(2) | 0.304 80(4) | 0.080 53(2) |

TABLE IV. Finite-volume corrections, $\Delta_{\rm vol} f$, to simulation results for the meson decay constants. Errors on the finite-volume correction come from our fit and are correlated between ensembles and between $\pi$ and $K$. Also listed for each ensemble are the lattice spacing $a$ (after determination of $w_0$ which gives the error shown, correlated between ensembles), the ratio of valence strange- to light-quark mass $m_s/m_\ell$, the spatial dimension of the lattice $L$, and the pion and kaon masses (with their statistical errors from Table III).

| $a$ | $m_s/m_\ell$ | $L$ | $M_\pi L$ | $M_\pi$ (MeV) | $M_K$ (MeV) | $\Delta_{\rm vol} f_\pi$ (%) | $\Delta_{\rm vol} f_K$ (%) | $\Delta_{\rm vol} f_{\eta_s}$ (%) |
|---|---|---|---|---|---|---|---|---|
| 0.1543(8) fm | 5.3 | 2.5 fm | 3.8 | 302.4(2) | 527.1(3) | 1.24(23) | 0.50(9) | 0.10(0) |
| 0.1522(8) fm | 10.6 | 3.7 fm | 4.0 | 215.5(1) | 506.8(1) | 0.38(7) | 0.12(2) | 0.00(0) |
| 0.1509(8) fm | 26.7 | 4.8 fm | 3.3 | 133.0(1) | 477.9(1) | 0.43(8) | 0.13(2) | 0.00(0) |
| 0.1241(7) fm | 5.0 | 3.0 fm | 4.6 | 304.5(1) | 521.2(2) | 0.37(7) | 0.14(3) | 0.01(0) |
| 0.1223(6) fm | 10.0 | 3.9 fm | 4.3 | 216.5(1) | 496.4(2) | 0.24(5) | 0.08(1) | 0.00(0) |
| 0.1212(6) fm | 27.6 | 5.8 fm | 3.9 | 132.7(0) | 485.7(1) | 0.15(3) | 0.05(1) | 0.00(0) |
| 0.0907(5) fm | 4.9 | 2.9 fm | 4.5 | 306.1(2) | 520.6(2) | 0.41(8) | 0.16(3) | 0.02(0) |
| 0.0879(4) fm | 30.0 | 5.6 fm | 3.7 | 128.4(0) | 490.8(1) | 0.21(4) | 0.07(1) | 0.00(0) |

$$f_{\rm NLO}(x_a, x_b, x_\ell^{\rm sea}, x_s^{\rm sea}, L) + \delta f_\chi + \delta f_{\rm lat}. \tag{7}$$

Here $f_{\rm NLO}$ is the result from chiral perturbation theory through one-loop order, in a finite volume of size $L$ on a side, and $\delta f_\chi$ and $\delta f_{\rm lat}$ are corrections for higher-order chiral contributions and nonzero lattice-spacing errors, respectively. We specify valence- and sea-quark masses through the dimensionless parameters $x_a$, $x_b$, etc., where, for example, a light quark with mass $m_\ell = (m_u + m_d)/2$ would correspond to

$$x_\ell = \frac{M_{0,\pi}^2}{16\pi^2 f_0^2}. \tag{8}$$

Here $f_0$ is fixed to the standard value 131.5 MeV, close to the experimental result for $f_\pi$. $M_{0,\pi}$ is the bare pion mass obtained by subtracting the one-loop chiral correction from masses measured in the simulation (Table III). Using bare meson masses corrects for (negligible) finite-volume errors in the masses. The $s$-quark parameter is given by

$$x_s = \frac{2M_{0,K}^2 - M_{0,\pi}^2}{16\pi^2 f_0^2}, \tag{9}$$

where $M_{0,K}$ is the bare mass coming from the kaon masses measured in the simulation. The same formula is used for each of the three mesons we study, changing only the valence masses:

$$\begin{aligned} f_\pi &\leftrightarrow f_{\rm NLO}(x_\ell, x_\ell, x_\ell^{\rm sea}, x_s^{\rm sea}, L) + \delta f_\chi + \delta f_{\rm lat}, \\ f_K &\leftrightarrow f_{\rm NLO}(x_\ell, x_s, x_\ell^{\rm sea}, x_s^{\rm sea}, L) + \delta f_\chi + \delta f_{\rm lat}, \\ f_{\eta_s} &\leftrightarrow f_{\rm NLO}(x_s, x_s, x_\ell^{\rm sea}, x_s^{\rm sea}, L) + \delta f_\chi + \delta f_{\rm lat}. \end{aligned} \tag{10}$$

In our fits, we use very broad priors for the chiral parameters in $f_{\rm NLO}$—10–100 times wider than the final errors—so these have no impact on the fit. We also introduce a new parameter that multiplies the finite-volume correction in $f_{\rm NLO}$. This allows our fit to correct (crudely) for finite-volume corrections from higher orders in chiral perturbation theory. We set its prior to $1 \pm 0.33$. Finite-volume corrections are quite small on almost all of the ensembles, as is evident from Table IV which lists corrections for the decay constants. (The $\eta_s$ mass has very small corrections, similar in magnitude to those for $f_{\eta_s}$.) The finite-volume corrections agree at the level of the errors we have with the range of those calculated in [25], as well as with the finite-volume analysis in [10].

The square of the $\eta_s$ mass is fit with an analogous formula of the form

$$M_{\rm NLO}^2(x_a, x_b, x_\ell^{\rm sea}, x_s^{\rm sea}, L) + \delta M_\chi^2 + \delta M_{\rm lat}^2, \tag{11}$$

with $x_a = x_b = x_s$.

### B. Higher-order corrections

We include terms beyond one-loop order in chiral perturbation theory by adding a correction of the form

$$\begin{aligned} \delta f_\chi \equiv\ & c_{2a}(x_a + x_b)^2 + c_{2b}(x_a - x_b)^2 + c_{2c}(x_a + x_b)(2x_\ell^{\rm sea} + x_s^{\rm sea}) + c_{2d}(2x_\ell^{\rm sea} + x_s^{\rm sea})^2 + c_{2e}(2x_\ell^{\rm sea2} + x_s^{\rm sea2}) + c_{3a}(x_a + x_b)^3 \\ & + c_{3b}(x_a + x_b)(x_a - x_b)^2 + c_{3c}(x_a + x_b)^2(2x_\ell^{\rm sea} + x_s^{\rm sea}) + c_4(x_a + x_b)^4 + c_5(x_a + x_b)^5 + c_6(x_a + x_b)^6, \end{aligned} \tag{12}$$

where we take priors of $0 \pm 1$ for each parameter $c_j$. We only keep higher-order terms that might be significant given the precision of our simulation data. In fact, we obtain an excellent fit and almost identical results (to within a quarter of a standard deviation) when we keep only the quadratic terms. We include an analogous correction, $\delta M_\chi^2$, for the square of the $\eta_s$ mass.

We also correct for the nonzero lattice spacing using

$$\delta f_{\rm lat} \equiv \sum_{n=1}^{4} d_n \left(\frac{a\Lambda_{\rm QCD}}{\pi}\right)^{2n}, \tag{13}$$

where $d_n$ is allowed to depend upon the quark masses,

$$d_n = d_{n,0} + d_{n,1a}(x_a + x_b) + d_{n,1b}(2x_\ell^{\rm sea} + x_s^{\rm sea}) + d_{n,1c}(x_a + x_b)^2, \quad (14)$$

and again the coefficients have priors $0 \pm 1$. We get excellent fits and almost identical answers without allowing for mass dependence, but we are conservative and include this possibility, since it could arise from taste-changing effects [18,26], thereby increasing our final errors by about half a standard deviation.

Equation (13) is an expansion in the QCD scale $\Lambda_{\rm QCD}$ divided by the ultraviolet cutoff, $\pi/a$, for the lattice. The QCD scale is of order 500 MeV to 1 GeV. This is confirmed by the empirical Bayes criterion [19] which shows that our data imply a scale of about 600 MeV. In our analysis we use a conservative value, 1.8 GeV, to ensure that nonzero lattice-spacing errors are not underestimated.

### C. Isospin violation and electromagnetism

We need to determine the $x_\ell$ and $x_s$ values corresponding to physical pion and kaon masses if we are to use our formulas to extract physical values for the decay constants and the $\eta_s$ mass. The correct pion and kaon masses come from experiment, but there are two complications that result from simplifications in the simulations. The first is that the simulation does not include electromagnetism. The second is that $m_u = m_d$ in the simulation, while in reality $m_u = 0.48(10)m_d$ [1].

The most appropriate pion mass for $f_{\pi^+}$ is the neutral-pion mass [134.9766(6) MeV [1]]. All $\pi$ mesons would have this mass in a world without electromagnetism—our simulations, for example—up to very small (quadratic) corrections from the $u$-$d$ mass difference. These corrections are estimated at 0.32(20) MeV for $M_{\pi^+}$ in [27]. For our purposes, it is sufficient to take 0.32 MeV as the uncertainty in the pion mass, and ignore the distinction between charged and neutral pions:

$$M_\pi^{\rm phys} = 134.98(32)\ {\rm MeV}. \quad (15)$$

This pion mass corresponds in our simulation to a light-quark mass of $m_\ell = (m_u + m_d)/2$. The corresponding kaon mass is one for an $s\bar{\ell}$ meson. This is the root-mean-square average of the $K^+$ and $K^0$ masses with additional small corrections for electromagnetism:

$$(M_K^{\rm phys})^2 \equiv \frac{1}{2}[(M_{K^+}^2 + M_{K^0}^2) - (1 + \Delta_E)(M_{\pi^+}^2 - M_{\pi^0}^2)]. \quad (16)$$

$\Delta_E$ would be zero if electromagnetic effects in the $K$ system mirrored those of the $\pi$. In fact it is closer to 1. Recent lattice calculations [28–30] that include electromagnetic effects give values in the region 0.6–0.7. We take $\Delta_E = 0.65(50)$ to conservatively encompass these results and this gives

$$M_K^{\rm phys} = 494.6(3)\ {\rm MeV}. \quad (17)$$

Tuning the pion mass to $M_\pi^{\rm phys}$ and the kaon mass to $M_K^{\rm phys}$ in our fits sets the strange-quark mass to its physical value, and the light-quark mass to the average $m_\ell$ of the $u$ and $d$ masses. This light-quark mass is correct, to within our errors, for the valence quarks in the pion, and for sea quarks in all three mesons.

This tuning is not correct, however, for the $K^+$'s valence light quark, which is a $u$ quark, with mass $0.65(9)m_\ell$. This difference produces a small but significant downward shift in $f_{K^+}$. To compute the corrected $K^+$ decay constant, we evaluate our fit formulas with a pion mass given by $\sqrt{0.65(9)}M_\pi^{\rm phys}$, while adjusting the kaon mass so that $2M_K^2 - m_\pi^2$ is unchanged (to leave the $s$-quark mass unchanged). These adjustments are made only for the valence-quark masses in the $K^+$; the valence-quark masses in the pion and $\eta_s$, as specified by $M_\pi^{\rm phys}$ and $M_K^{\rm phys}$, are left unchanged, as are the sea-quark masses in each of the mesons.

### D. Fit results

We fit $w_0$ times each of the decay constants and each $\eta_s$ mass in Table III to the formulas above, as functions of the pion and kaon masses and $w_0$. We also fit the experimental value for $f_{\pi^+} = 130.4(2)$ MeV to our formula evaluated at the physical pion and kaon masses, Eqs. (15) and (17). These fits are all done simultaneously using the same parameters for the fit functions in each case, and including the correlations between $\pi$, $K$, and $\eta_s$ results discussed in Sec. II.

The results for the decay constants as a function of the light-quark mass are shown in Fig. 3. For each decay constant we show fit results and simulation data for each of our three lattice spacings. The dashed line shows the continuum extrapolation, while the grey band shows our final results extrapolated to zero lattice spacing and the physical light-quark mass limit (with the light-quark mass equal to the $u$-$d$ average). The fit is excellent with a $\chi^2$ per degree of freedom of 0.42 ($p$ value 0.99), fitting 39 pieces of data. There are 61 parameters, each with a Bayesian prior. The final results are

$$\begin{aligned} f_\pi &= 130.39(20)\,{\rm MeV}, & f_{K^+}/f_{\pi^+} &= 1.1916(21), \\ f_{K^+} &= 155.37(34)\,{\rm MeV}, & f_{\eta_s}/M_{\eta_s} &= 0.2631(11), \\ f_{\eta_s} &= 181.14(55){\rm MeV}, & M_{\eta_s}^2/(2M_K^2 - M_\pi^2) &= 1.0063(64), \\ M_{\eta_s} &= 688.5(2.2)\,{\rm MeV}, & f_{\eta_s}/(2f_K - f_\pi) &= 0.9997(17), \\ & & w_0 &= 0.1715(9)\,{\rm fm}. \end{aligned} \quad (18)$$

Clearly the result for $f_\pi$ contains no new information beyond the input value from the experiment that was included as a fit parameter. The $K^+$ results here are adjusted to correct the valence light-quark mass, as discussed above. We find that the $K^+$ decay constant is 0.27(7)%

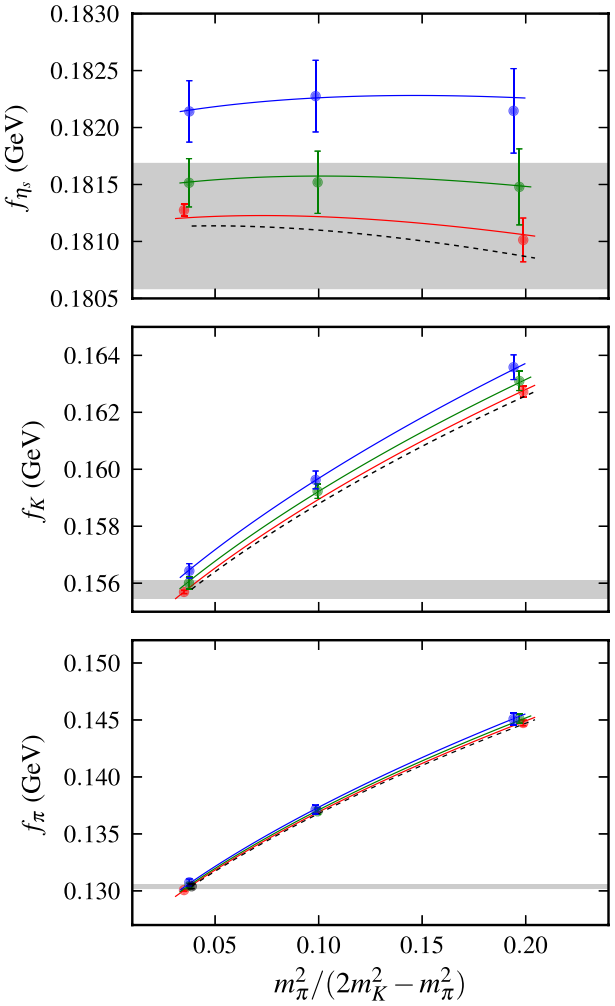


FIG. 3 (color online). Fit results for the $\pi$, $K$, and $\eta_s$ decay constants as functions of the light-quark mass for three different lattice spacings: 0.15 fm (top/blue), 0.12 fm (middle/green), and 0.09 fm (bottom/red). The data shown are from Table III, with corrections for errors in the $s$ masses, and for finite-volume errors. The lines show our fit with the best-fit values of the fit parameters. The dashed line is the $a = 0$ extrapolation, and the grey band shows our continuum results at the physical light-quark mass point with $m_\ell = (m_u + m_d)/2$. The current experimental result for $f_{\pi^+}$ is also shown (black point). Note that the three plots are against very different scales in the vertical direction: the range covered in the $f_\pi$ plot is 10 times larger than that covered in the $f_{\eta_s}$ plot.

lower than the decay constant for a kaon whose valence light-quark's mass equals the $u$-$d$ average mass.

Error budgets for several of our results are presented in Table V. Our fits are unchanged if we include additional higher-order chiral or $a^2$ corrections, beyond what is discussed above. Omitting results from any one of our configuration sets shifts the mean values by no more than one standard deviation and usually much less. Omitting results from the smallest lattice spacing (0.09 fm) gives the same mean values but with standard deviations that are 2.5 times larger. Omitting the most chiral results ($m_s/m_l > 25$) shifts

TABLE V. Sources of uncertainty in the final results [Eq. (18)] for the $K^+$ decay constant, the ratio of $K^+$ to $\pi^+$ decay constants, the $\eta_s$ mass, and the Wilson flow parameter $w_0$.

| | $f_{K^+}$ | $f_{K^+}/f_{\pi^+}$ | $m_{\eta_s}$ | $w_0$ |
|---|---|---|---|---|
| Statistics + svd cut | 0.13% | 0.13% | 0.28% | 0.26% |
| Chiral extrapolation | 0.03 | 0.03 | 0.04 | 0.15 |
| $a^2 \to 0$ extrapolation | 0.10 | 0.10 | 0.15 | 0.27 |
| Finite volume correction | 0.01 | 0.01 | 0.01 | 0.02 |
| $w_0/a$ uncertainty | 0.02 | 0.02 | 0.02 | 0.28 |
| $f_{\pi^+}$ experiment | 0.13 | 0.03 | 0.07 | 0.19 |
| $m_u/m_d$ uncertainty | 0.07 | 0.07 | 0.00 | 0.00 |
| Total | 0.22% | 0.18% | 0.33% | 0.54% |

the means by about 1/3 of a standard deviation and increases the standard deviation by 50%. These last two tests are evidence that our $a^2$ and chiral extrapolations are stable and robust.

As a check of the "statistical + svdcut"elements of the error budget we repeated the analysis using correlator results binned over many more adjacent configurations. We used a bin size of 16 corresponding to 80 molecular dynamics time units (64 or 96 on set 8 depending on stream). This gives the same final result within $0.5\sigma$ and the same errors.

The $a^2$ variation of our simulation results is quite small (1–2 standard deviations) across our entire range of lattice spacings. This is illustrated in Fig. 4 where we show simulation results for $f_K/f_\pi$ in the physical light-quark mass limit for our three lattice spacings (top curve); the grey band is the $a = 0$ result. This behavior is in marked contrast with what we obtain if we set the lattice spacing

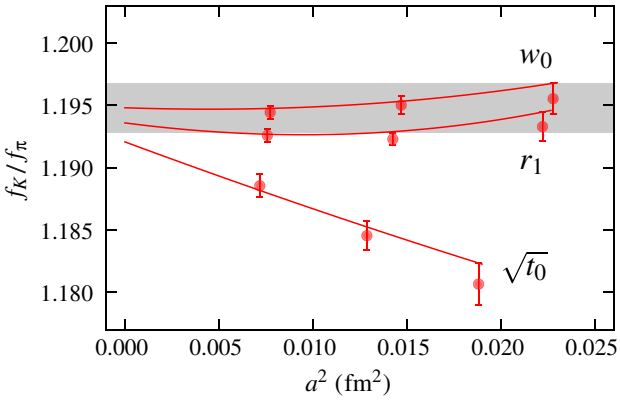


FIG. 4 (color online). Fit results for $f_K/f_\pi$ evaluated at the physical light-quark mass limit, with $m_\ell = (m_u + m_d)/2$, for different lattice spacings. The data shown are from Table III, with corrections for errors in the quark masses, and for finite-volume errors. The top curve and data are from our analysis using $w_0$ to set the lattice spacing; the middle results are from our analysis using $r_1$ instead of $w_0$; the bottom results are from our analysis using $\sqrt{t_0}$. The grey band shows the final result from the $w_0$ analysis.

using $\sqrt{t_0}$ (bottom curve). The two methods agree to within 1.3 standard deviations when extrapolated to $a = 0$, but the variation with $a^2$ in the $\sqrt{t_0}$ analysis is much larger. This agrees with the findings of [13] that $\sqrt{t_0}$ has larger discretization errors than $w_0$ when compared to hadronic quantities. We have also redone our analysis using $r_1$ (middle curve). These results are similar to those from the $w_0$ analysis, and give an extrapolated value that agrees with that analysis to within half a standard deviation. These two analyses also give

$$\sqrt{t_0} = 0.1420(8)\ \text{fm}, \qquad r_1 = 0.3112(30)\ \text{fm}. \tag{19}$$

We use quite broad priors for $w_0$, $\sqrt{t_0}$, and $r_1$ in our fits: 0.1755(175), 0.1400(140), and 0.3150(320), respectively. They have little effect on the fit results.

Finally, we give the Gasser-Leutwyler low-energy constants from the next-to-leading order (NLO) term in our chiral fit. These are evaluated at scale $M_\eta$ and given in units of $10^{-3}$:

$$\begin{aligned} L_4 &= 0.36(34), & L_6 &= 0.32(20), \\ L_5 &= 2.00(25), & L_8 &= 0.77(15), \\ 2L_6 - L_4 &= 0.28(17), & 2L_8 - L_5 &= -0.46(20). \end{aligned} \tag{20}$$

The values agree well with other chiral analyses, for example the MILC analysis on configurations including $u$, $d$, and $s$ asqtad sea quarks [31]. The errors on the low-energy constants reflect the fact that we allow for higher-order terms beyond NLO chiral perturbation theory in our fits.

Chiral extrapolation contributes much less to our error budget here than in our previous analyses. This is expected because we have lattice results for $m_\ell$ very close to the physical mass; indeed, $m_\ell$ is actually slightly below the physical mass, so we are interpolating. We checked our chiral extrapolation in several ways:

(i) We replaced the fixed value of $f_0$ that sets the chiral scale in Eqs. (8) and (9) with the floating parameter that corresponds to $f_\pi$ in the chiral limit. Any changes should be absorbed by the higher-order mass-dependent terms in the chiral fit, so this tests whether we have included enough higher-order terms. Changing $f_0$ in this way had negligible effect on our final answers (around $\sigma/20$).

(ii) We replaced SU(3) chiral perturbation theory with SU(2) chiral perturbation theory, where the chiral parameters for pions, kaons, and the $\eta_s$ are allowed to differ. Unlike in the SU(3) case, it is possible to fit our data with the SU(2) theory expanded only through NLO; the results are the same as above to within $1\sigma$, with slightly smaller errors. We prefer to include analytic terms from next-to-next-to-leading order and above to ensure that we have not underestimated our errors. This again gives results that agree with those in Eq. (18) (to better than $0.5\sigma$) but now with slightly larger errors (by $0.1\sigma$). See [31,32] for a comparison of SU(2) and SU(3) chiral fits with similar conclusions for results with asqtad $u$, $d$, and $s$ sea quarks.

(iii) We repeated our analysis using staggered chiral perturbation theory through one loop [26] supplemented by higher-order terms in meson masses and discretization effects, as given earlier in Eqs. (7), (12), and (13). Staggered chiral perturbation theory explicitly incorporates discretization effects that arise when using staggered quarks because of the multiple tastes of mesons that can appear in loop terms in the chiral expansion. The standard chiral logarithm terms are modified to include multiple tastes and in addition there are "hairpin" correction terms that also depend on taste splittings. The final effect from these two terms is very benign, even at physical quark masses. We find that final results from our fits differ by less than $0.5\sigma$ from the results given above in Eq. (18).

These tests give us confidence that our estimates of the errors due to our chiral fits are reliable.

## IV. DISCUSSION

Equation (18) lists a number of outputs from our analysis. The key result is that for $f_{K^+}$ and in particular the ratio $f_{K^+}/f_{\pi^+}$ needed to make use of Eq. (2). This is obtained with an error of 0.18%.

Figure 5 compares our new result for $f_{K^+}/f_{\pi^+}$ to earlier values on $n_f = 2 + 1 + 1$ ($u$, $d$, $s$, and $c$ sea quarks) [10] and $n_f = 2 + 1$ ($u$, $d$, $s$ sea quarks) configurations [5–9]. There is good agreement with earlier results within their

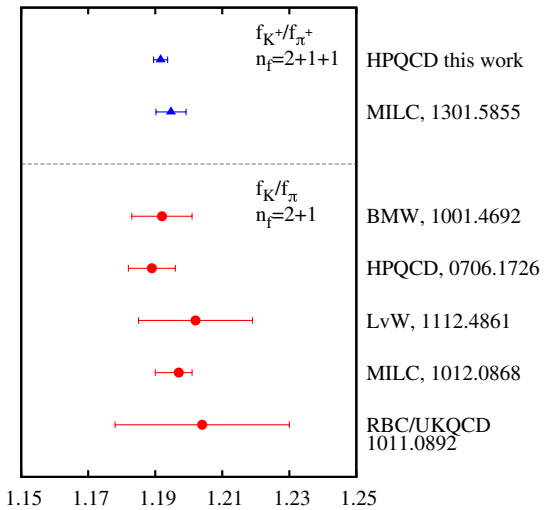


FIG. 5 (color online). A comparison of lattice QCD results for the ratio of $K$ to $\pi$ decay constants. The top two values (filled blue triangles) are for $f_{K^+}/f_{\pi^+}$ including $u$, $d$, $s$, and $c$ sea quarks—results from this paper and from [10]. The lower values (red squares) include $u$, $d$, and $s$ sea and typically do not distinguish $f_{K^+}$ from $f_K$ [5–9].

larger error bands. Typically the results on $n_f = 2 + 1$ did not distinguish between $f_{K^+}$ and $f_K$ because the errors were not small enough to see this difference. The difference that we see, 0.27(7)%, is in agreement with that expected from chiral perturbation theory [0.21(6)% [3]]. It is also in agreement with a simple-minded argument assuming that the ratio of $f_{\eta_s}/f_K$ depends linearly on $M_\pi^2$ between 0 and $M_{\eta_s}^2$.

Our result for $f_{K^+}/f_{\pi^+}$ is more accurate than MILC's recent analysis [10] based on the physical point ensembles because we have included additional information: accurate relative lattice-spacing values, fits to decay constants at heavier sea- and valence-quark masses, fits to $\eta_s$ masses and decay constants, and chiral perturbation theory to relate all of these fits at all of the lattice spacings to each other. The MILC error is dominated by their continuum extrapolation. Our Figs. 3 and 4 show very little dependence on lattice spacing (when using $w_0$) and benign extrapolations. Our error is nevertheless also dominated by the continuum extrapolation uncertainties along with statistical errors.

Our analysis also gives results for the properties of the $\eta_s$ meson, by fixing its mass and decay constant in the continuum and physical light-quark mass limits from those of the $\pi$ and $K$. Here the surprising result found earlier in [18] is how closely the properties of the $\eta_s$ match those expected from low-order chiral perturbation theory. Our results here agree well with earlier results from $n_f = 2 + 1$ [18] as well as from earlier analysis on these $n_f = 2 + 1 + 1$ configurations [16].

We used $w_0/a$ to determine the relative lattice spacing between ensembles. Fixing the lattice spacing finally from $f_\pi$ gives a physical value for $w_0$ in Eq. (18) of 0.1715(9) fm. This agrees at $2\sigma$ with the earlier result from BMW-c [13] of 0.1755(18) fm using the mass of the $\Omega$ baryon to fix the physical value. The error in the BMW-c result is dominated by the statistical errors in the lattice calculation of $M_\Omega$, and so we are able to obtain a smaller error using $f_\pi$.

In separate fits for comparison, not used for our central values, we also obtained values for $\sqrt{t_0}$ and $r_1$ in Eq. (19). Our $\sqrt{t_0}$ agrees with the value in [13]. The value for $r_1$ is not in good agreement with our earlier result, which it supersedes, on a subset of these ensembles [16], however. The reason for this is largely because the values for $r_1/a$ have been updated, resulting in changes outside the original error bars. This underscores the difficulty of determining parameters from the heavy-quark potential accurately [13] and provides further incentive to use $w_0$.

## V. CONCLUSIONS

We give here the most accurate result to date for $f_{K^+}/f_{\pi^+}$ from lattice QCD. Our result comes from "second-generation" gluon field configurations with a highly improved discretization of QCD and including $u$, $d$, $s$, and $c$ quarks in the sea. We fit results from a range of ensembles with $u/d$ quark masses down to the physical point and including additional accurate information on the relative lattice spacing between the ensembles. We test the robustness of our continuum extrapolation using two different methods for lattice-spacing determination. These features mean that we are able to improve on the error obtained by the MILC Collaboration [10] which aimed for a self-contained analysis using only physical $u/d$ quark masses.

Our result is

$$\frac{f_{K^+}}{f_{\pi^+}} = 1.1916(21). \tag{21}$$

With this level of accuracy the difference between $f_K$ with $m_u = m_d$ and $f_{K^+}$, which we determine to be 0.27(7)%, is important. Going forward it will be necessary to make sure that $f_K$ and $f_{K^+}$ results from lattice QCD are averaged separately.

Using Eq. (2) we determine

$$\frac{|V_{us}|}{|V_{ud}|} = 0.23160(29)_{\mathrm{Br}(K^+)}(21)_{\mathrm{EM}}(41)_{\mathrm{latt}}. \tag{22}$$

It is no longer true that the lattice QCD error is much larger than the total of experiment plus corrections to experiment from electromagnetism.

Given a value of $V_{ud}$ from nuclear $\beta$ decay of 0.974 25 (22) [33] gives

$$|V_{us}| = 0.22564(28)_{\mathrm{Br}(K^+)}(20)_{\mathrm{EM}}(40)_{\mathrm{latt}}(5)_{V_{ud}}. \tag{23}$$

This agrees well with values from experimental results for semileptonic $K$ decay rates combined with lattice QCD calculations of the appropriate hadronic form factor [2,34,35]. The test of unitarity of the first row of the CKM matrix yields $1 - |V_{ud}|^2 - |V_{us}|^2 - |V_{ub}|^2 = -0.000\,09(51)$. This agrees well with the Standard Model result of zero and pushes the scale of new physics above 10 TeV [36]. To improve the limit on this scale significantly now needs further improvements to the accuracy of $V_{ud}$ [33].

## ACKNOWLEDGMENTS

We are grateful to the MILC Collaboration for the use of their gauge configurations and to R. van de Water for useful discussions. We have used the MILC code for some of our propagator calculations. The results described here were obtained using the Darwin Supercomputer of the University of Cambridge High Performance Computing Service as part of STFC's DiRAC facility. We are grateful to the Darwin support staff for assistance. This work was funded by DFG (Grant No. SFB-TR 55), NSF, the Royal Society, the Wolfson Foundation, and STFC.

[1] J. Beringer *et al.* (Particle Data Group), Phys. Rev. D **86**, 010001 (2012).
[2] M. Antonelli, V. Cirigliano, G. Isidori, F. Mescia, M. Moulson *et al.*, Eur. Phys. J. C **69**, 399 (2010).
[3] V. Cirigliano and H. Neufeld, Phys. Lett. B **700**, 7 (2011).
[4] W. J. Marciano, Phys. Rev. Lett. **93**, 231803 (2004).
[5] E. Follana, C. Davies, G. Lepage, and J. Shigemitsu (HPQCD Collaboration and UKQCD Collaboration), Phys. Rev. Lett. **100**, 062002 (2008).
[6] S. Dürr, Z. Fodor, C. Hoelbling, S. D. Katz, S. Krieg, T. Kurth, L. Lellouch, T. Lippert, A. Ramos, and K. K. Szabó, Phys. Rev. D **81**, 054507 (2010).
[7] A. Bazavov *et al.* (MILC Collaboration), Proc. Sci., LATTICE2010 (2010) 074 [arXiv:1012.0868].
[8] Y. Aoki *et al.* (RBC Collaboration and UKQCD Collaboration), Phys. Rev. D **83**, 074508 (2011).
[9] J. Laiho and R. S. Van de Water, Proc. Sci., LATTICE2011 (2011) 293 [arXiv:1112.4861].
[10] A. Bazavov, C. Bernard, C. DeTar, J. Foley, W. Freeman *et al.* (MILC Collaboration), Phys. Rev. Lett. **110**, 172003 (2013).
[11] E. Follana, Q. Mason, C. Davies, K. Hornbostel, G. Lepage, J. Shigemitsu, H. Trottier, and K. Wong (HPQCD Collaboration), Phys. Rev. D **75**, 054502 (2007).
[12] A. Hart, G. M. von Hippel, and R. R. Horgan (HPQCD Collaboration), Phys. Rev. D **79**, 074008 (2009).
[13] S. Borsanyi, S. Durr, Z. Fodor, C. Hoelbling, S. D. Katz *et al.*, J. High Energy Phys. 09 (2012) 010.
[14] A. Bazavov *et al.* (MILC Collaboration), Phys. Rev. D **82**, 074501 (2010).
[15] A. Bazavov *et al.* (MILC Collaboration), Phys. Rev. D **87**, 054505 (2013).
[16] R. Dowdall *et al.* (HPQCD Collaboration), Phys. Rev. D **85**, 054509 (2012).
[17] C. McNeile, A. Bazavov, C. T. H. Davies, R. J. Dowdall, K. Hornbostel, G. P. Lepage, and H. D. Trottier, Phys. Rev. D **87**, 034503 (2013).
[18] C. Davies, E. Follana, I. Kendall, G. Lepage, and C. McNeile (HPQCD Collaboration), Phys. Rev. D **81**, 034506 (2010).
[19] G. P. Lepage, B. Clark, C. T. H. Davies, K. Hornbostel, P. B. Mackenzie, C. Morningstar, and H. Trottier, Nucl. Phys. B, Proc. Suppl. **106–107**, 12 (2002).
[20] G. P. Lepage, https://github.com/gplepage.
[21] M. Luscher, J. High Energy Phys. 08 (2010) 071.
[22] R. Sommer, Nucl. Phys. **B411**, 839 (1994).
[23] A. Bazavov *et al.*, Rev. Mod. Phys. **82**, 1349 (2010).
[24] S. R. Sharpe and N. Shoresh, Phys. Rev. D **62**, 094503 (2000).
[25] G. Colangelo, S. Durr, and C. Haefeli, Nucl. Phys. **B721**, 136 (2005).
[26] C. Aubin and C. Bernard, Phys. Rev. D **68**, 074011 (2003).
[27] G. Amoros, J. Bijnens, and P. Talavera, Nucl. Phys. **B602**, 87 (2001).
[28] S. Basak *et al.* (MILC Collaboration), Proc. Sci., LATTICE2012 (2012) 137 [arXiv:1210.8157].
[29] A. Portelli, S. Durr, Z. Fodor, J. Frison, C. Hoelbling *et al.*, Proc. Sci., LATTICE2011 (2011) 136 [arXiv:1201.2787].
[30] T. Blum, R. Zhou, T. Doi, M. Hayakawa, T. Izubuchi, S. Uno, and N. Yamada, Phys. Rev. D **82**, 094508 (2010).
[31] A. Bazavov *et al.* (MILC Collaboration), Proc. Sci., LAT2009 (2009) 079 [arXiv:0910.3618].
[32] A. Bazavov *et al.* (MILC Collaboration), Proc. Sci., LAT2009 (2009) 077 [arXiv:0911.0472].
[33] J. Hardy and I. Towner, Phys. Rev. C **79**, 055502 (2009).
[34] A. Bazavov, C. Bernard, C. Bouchard, C. DeTar, D. Du *et al.* (MILC Collaboration), Phys. Rev. D **87**, 073012 (2013).
[35] P. A. Boyle, J. M. Flynn, A. Jüttner, C. Kelly, C. Maynard, H. Pedroso Lima, C. T. Sachrajda, and J. M. Zanotti (RBC-UKQCD Collaboration), Eur. Phys. J. C **69**, 159 (2010).
[36] V. Cirigliano, J. Jenkins, and M. Gonzalez-Alonso, Nucl. Phys. **B830**, 95 (2010).